

Certifying multiparticle entanglement with randomized measurements

Andreas Ketterer,^{1,2} Satoya Imai,³ Nikolai Wyderka,⁴ and Otfried Gühne³

¹*Physikalisches Institut, Albert-Ludwigs-Universität Freiburg,
Hermann-Herder-Straße 3, 79104 Freiburg, Germany*

²*EUCOR Centre for Quantum Science and Quantum Computing,
Albert-Ludwigs-Universität Freiburg, Hermann-Herder-Str. 3, 79104 Freiburg, Germany*

³*Naturwissenschaftlich-Technische Fakultät, Universität Siegen,
Walter-Flex-Straße 3, 57068 Siegen, Germany*

⁴*Institut für Theoretische Physik III, Heinrich-Heine-Universität Düsseldorf,
Universitätsstraße 1, 40225 Düsseldorf, Germany*

The presence of multiparticle entanglement is an important benchmark for the performance of intermediate-scale quantum technologies. In this work we consider statistical methods based on locally randomized measurements in order to characterize different degrees of multiparticle entanglement in qubit systems. We introduce hierarchies of criteria, satisfied by states which are separable with respect to partitions of different size, involving only second moments of the underlying probability distribution. Furthermore, we study in detail the resources required for a statistical estimation of the respective moments if only a finite number of samples is available, and discuss their scaling with the system size.

Introduction.— Intermediate-scale quantum devices involving a few dozen qubits are considered a stepping stone towards the ultimate goal of building a fault-tolerant quantum computer. While impressive achievements have been made in this direction, e.g., in terms of the precision of the individual qubit architectures [1–3], the common challenge is to scale up the considered devices and, at the same time, maintaining the established accuracy [4, 5]. In particular, the collective performance of the whole system of interacting qubits is of central concern in this respect. In order to gauge the performance of such devices methods that allow for a characterization of multiparticle correlations are indispensable.

Several approaches aiming at a verification of properties of multiparticle quantum systems have been discussed in the literature [6]. On the one hand, there are efficient protocols in terms of the required measurement resources if the experiment is expected to result in specific states, e.g., entanglement witnessing [7], self-testing [8] or direct fidelity estimation [9, 10]. On the other hand, approaches which rely on few or no expectation about the underlying quantum state are usually very resource-intensive and thus do not scale favorably with increasing system sizes, e.g., quantum state tomography [11, 12]. Furthermore, intermediate strategies exist which do not aim for a full mathematical description of the system but rather focus on specific sets of statistical properties. The latter can reduce the required measurement resources considerably at the expense of a non-vanishing statistical error and do not assume any prior information about the state [13–15].

Recently there has been much attention on protocols based on statistical correlations between outcomes of randomized measurements [16–31] (see Fig. 1). The latter allow to infer several properties of the underlying system, ranging from structures of multiparticle entangle-

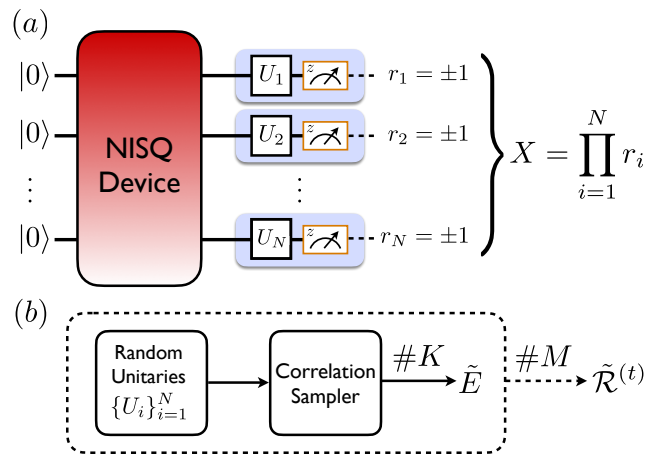


FIG. 1. Characterization of a noisy intermediate-scale quantum (NISQ) device through locally randomized measurements. (a) A measurement of N qubits in random local bases defined through the set of local unitary transformations $\{U_i\}_{i=1}^N$ resulting in a correlation sample X . (b) Repetition of the measurement protocol presented in (a) for M sets of randomly sampled measurement bases and K individual projective measurements per fixed measurement bases yields estimates of the moments (2).

ment [19, 20, 30], over subsystem purities [24, 25], to fidelities with respect to certain target states or even another quantum devices [13, 28]. At the core of all those approaches is the idea to perform measurements in randomly sampled local bases leading to ensembles of measurement outcomes whose distributions provide a fingerprint of the system's correlation properties. Concerning resources required for statistically significant tests, scaling properties have been derived for the case of bipartite entanglement [23, 29].

In this work we present a comprehensive approach to

certify multiparticle entanglement structures in systems consisting of many qubits. First, we derive criteria in terms of second moments of randomized measurements for different forms of multiparticle entanglement, such as genuine multiparticle entanglement or the entanglement depth. Second, based on the Chebyshev-Cantelli inequality, we present a rigorous approach for the statistical analysis of practical experiments with a finite number of samples. As we will see, our results may directly be used in current experiments using Rydberg atom arrays or superconducting qubits [32–34].

Moments of random correlations.— We consider a mixed quantum state of N qubits described by the density matrix ρ which might be the output of a noisy quantum computation. In order to characterize this state we follow a strategy based on locally randomized measurements. Each random measurement is characterized through a set of random bases $\{|u_n^{(0)}\rangle = U_n|0_n\rangle, |u_n^{(1)}\rangle = U_n|1_n\rangle\}_{n=1,\dots,N}$, with $\{U_n\}_{n=1,\dots,N}$ picked from the unitary group $U(2)$ according to the Haar measure μ . Further on, we can associate to each element $(|u_n^{(0)}\rangle = U_n|0_n\rangle, |u_n^{(1)}\rangle = U_n|1_n\rangle)$, with $n \in \{1, \dots, N\}$, a direction \mathbf{u}_n on the unit sphere S^2 with components $[\mathbf{u}_n]_i = \text{tr}[\sigma_{\mathbf{u}_n} \sigma_i]$, with $i \in \{x, y, z\}$, and $\sigma_{\mathbf{u}_n} = U_n \sigma_z U_n^\dagger$ (see Fig. 1(a)). One such random measurement then enables us to retrieve the correlation function:

$$E(\mathbf{u}_1, \dots, \mathbf{u}_N) = \langle \sigma_{\mathbf{u}_1} \otimes \dots \otimes \sigma_{\mathbf{u}_N} \rangle_\rho. \quad (1)$$

The correlation function (1) provides a random snapshot of the correlation properties of the output state ρ . In order to get a more complete picture we consider the corresponding moments

$$\mathcal{R}^{(t)} = \frac{1}{(4\pi)^N} \int_{S^2} d\mathbf{u}_1 \dots \int_{S^2} d\mathbf{u}_N [E(\mathbf{u}_1, \dots, \mathbf{u}_N)]^t, \quad (2)$$

where t is a positive integer and $d\mathbf{u}_i = \sin \theta_i d\theta_i d\phi_i$ denotes the uniform measure on the sphere S^2 . The moments (2) are by definition invariant under local unitary transformation, i.e., LU-invariant, and thus good candidates for the characterization of multiparticle correlations. In the following we will show that already the lowest non-zero moment $\mathcal{R}^{(2)}$ allows for the characterization of several instances of multiparticle entanglement.

Multiparticle entanglement characterization.— One way to infer the multiparticle entanglement properties of a quantum state is to show that its structure is incompatible with that of different types of separable states. In general, one defines k -separable states, with $k \in \{2, \dots, N\}$, as those states which cannot be written as a statistical mixture of k -fold product states $|\Psi^{(k)}\rangle = |\phi_1\rangle \otimes \dots \otimes |\phi_k\rangle$. Hence, by disproving that a quantum state belongs to the above separability classes one can infer different degrees of multiparticle entanglement, with the strongest form given by those states which are not

even 2-separable and commonly referred to as genuinely multiparticle entangled (GME).

It is known that N -separable (i.e. fully-separable) states fulfill the bound $\mathcal{R}^{(2)} \leq 1/3^N$ [17, 18], a result that had previously been recognized in the context of reference-frame-independent entanglement detection [35–38]. Furthermore, bi-separability bounds on combinations of second moments of marginals of three-qubit systems can be formulated [30, 39]. However, so far no useful bounds on the full N -qubit moments (2) for the detection of genuine multiparticle entanglement have been found. Here we close this gap and prove in App. ID that all k -separable mixed states fulfill the bounds

$$\mathcal{R}^{(2)} \leq \frac{1}{3^{N-k+1}} \times \begin{cases} 2^{N-(2k-1)}, & N \text{ odd}, \\ 2^{N-(2k-1)} + 1, & N \text{ even}, \end{cases} \quad (3)$$

with $k = 2, \dots, \lfloor (N-1)/2 \rfloor$. Equation (3) thus provides a hierarchy of entanglement criteria whose violation for fixed k implies that the given state is at most $(k-1)$ -separable. This implies that it has an entanglement depth [40, 41] of at least $\lceil N/(k-1) \rceil$, but possibly stronger bounds for the depth can be derived based on the concept of producibility, see App. IE. In any case, only states which are GME can reach the maximum value of the second moment $\mathcal{R}^{(2)}$ which is known to be attained by the N -qubit GHZ states [42, 43]:

$$\mathcal{R}_{|\text{GHZ}_N\rangle}^{(2)} = \frac{1}{3^N} \times \begin{cases} 2^{N-1}, & N \text{ odd}, \\ 2^{N-1} + 1, & N \text{ even}. \end{cases} \quad (4)$$

with $|\text{GHZ}_N\rangle = (|0\rangle^{\otimes N} + |1\rangle^{\otimes N})/\sqrt{2}$. Note that in systems consisting of larger local dimensions it is in general not true that states which maximize the corresponding generalized second moment $\mathcal{R}^{(2)}$ are GME [30, 42, 43].

In order to study the performance of the criteria (3) we consider in the following the noisy N -qubit GHZ states $\rho_{\text{GHZ}}^{(N)}(p) := p\mathbb{1}/2^N + (1-p)|\text{GHZ}_N\rangle\langle\text{GHZ}_N|$, which yields $\mathcal{R}_{\text{GHZ}}^{(2)}(p, N) = (1-p)^2 \mathcal{R}_{|\text{GHZ}_N\rangle}^{(2)}$ and thus for $p=0$ and $p=1$ attains the minimum and maximum of $\mathcal{R}^{(2)}$, respectively. For each N , we can now calculate the threshold value of p up to which the criteria (3) are violated as a function of the parameter k , yielding

$$p^* = 1 - f(N, k) \left(\frac{3}{4} \right)^{\frac{k-1}{2}}, \quad (5)$$

where $f(N, k) = 1$ for odd N and $f(N, k) = \sqrt{(4^k + 2^{N+1})/(4 + 2^{N+1})}$ for even N . The functional behaviour of the threshold values (5) is illustrated in Fig. 2 as a function of k and the qubit number N . In the case of odd N , as becomes clear from Eq. (5), the threshold p^* is independent of the number of qubits N and coincides with the asymptotic threshold in the limit $N \rightarrow \infty$, where $f(N, k) \rightarrow 1$. Hence, as the asymptotic thresholds of p^* are strictly smaller than 1, our criteria (3) allow for the detection of multiparticle entanglement even

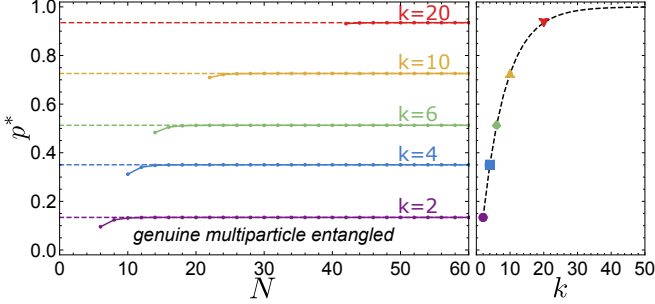


FIG. 2. Left: Threshold value p^* up to which the noisy GHZ state $\rho_{\text{GHZ}}^{(N)}(p)$ is detected to be not 2- (violet, bottom), 4- (blue), 6- (green), 10- (yellow) and 20-separable (red, top) as a function of the number of qubits N . While dots connected by solid lines represent values of p^* for even N , dashed lines correspond to the case of odd N which also represent the asymptotic values in the limit $N \rightarrow \infty$. Right: Plot of the asymptotic values of p^* in the limit aforementioned limit as a function of the parameter k . The exemplary values of the left plot are highlighted by colored markers, respectively.

in systems consisting of a large number of qubits. Furthermore, these methods also work for low fidelities, i.e., large p^* 's, and thus can also be applied in regimes where fidelity-based witnesses fail (see Fig. 2(right)). Lastly, we note that the criteria (3) become useful only for a certain minimum number of qubits depending on the value of k , e.g., GME detection is only possible for $N > 4$. In conclusion, the above introduced methods demonstrate their potential mainly in large multiparticle systems where an estimation of the required measurement resources is crucial.

Estimation of the moments.— In order to estimate the above moments we assume in the following that a finite sample of M random measurement bases is taken, each of which undergoes K individual projective measurements. We thus denote the individual outcomes of a single random measurement on N qubits by $\{r_1, \dots, r_N\}$, with $r_i = \pm 1$, and define the corresponding correlation sample as $X = \prod_{i=1}^N r_i$ (see Fig. 1(a)). Given a fixed measurement basis we can thus model the binary outcomes of X through a binomially distributed random variable \tilde{Y} with probability P , i.e., the probability that an even number of the measurement outcomes r_i result in -1 , and K trials. The corresponding unbiased estimators \tilde{P}_k of P and its k -th powers, respectively, are then given by $\tilde{P}_k = \tilde{P}_{k-1} [K\tilde{P}_1 - (k-1)]/[K - (k-1)]$, with $\tilde{P}_1 = \tilde{Y}/K$ (see App. II A).

Further on, the unbiased estimators of the respective t -th powers of Eq. (1) read

$$\tilde{E}_t = (-1)^t \sum_{k=0}^t (-2)^k \binom{t}{k} \tilde{P}_k \quad (6)$$

which, in turn, allows us to define faithful estimators of

the moments (2), resulting from M sampled measurement bases:

$$\tilde{\mathcal{R}}^{(t)} = \frac{1}{M} \sum_{i=1}^M [\tilde{E}_t]_i. \quad (7)$$

Given Eqs. (6) and (7), our goal is now to gauge the statistical error of an estimation $\tilde{\mathcal{R}}^{(t)}$ as a function of the number of subsystems N . More precisely, we aim for lower bounds on the total number of required measurement samples $M_{\text{tot}} = M \times K$ needed in order to estimate $\mathcal{R}^{(t)}$ with a precision of at least δ and confidence γ , i.e., such that $\text{Prob}(|\tilde{\mathcal{R}}^{(t)} - \mathcal{R}^{(t)}| \leq \delta) \geq \gamma$ for $M_{\text{tot}} \geq M(\gamma, t)$.

Here, the Chebyshev-Cantelli inequality comes into play, as it gives a bound on the deviation probability in terms of the variance [44]. From that we find that the precision δ up to which the moments $\mathcal{R}^{(t)}$ can be evaluated satisfies the bound:

$$\delta \leq \sqrt{\frac{1+\gamma}{1-\gamma} \text{Var}(\tilde{\mathcal{R}}^{(t)})}, \quad (8)$$

where $\text{Var}(\tilde{\mathcal{R}}^{(t)})$ denotes the variance of the estimator (7) which can be evaluated using the properties of the binomial distribution. For instance, in case of the second moment $\mathcal{R}^{(2)}$ we find that the variance reads

$$\text{Var}(\tilde{\mathcal{R}}^{(2)}) = \frac{1}{M} \left[A(K) \mathcal{R}^{(4)} + B(K) \mathcal{R}^{(2)} + C(K) - (\mathcal{R}^{(2)})^2 \right], \quad (9)$$

with $A(K) = (K-2)(K-1)C(K)/2$, $B(K) = 2(K-2)C(K)$ and $C(K) = 2/[K(K-1)]$ which are determined through the properties of the binomial distribution (see App. II A for a derivation).

Hence, the precision of an estimation of the second moment is determined through Eq. (8) and (9) and thus depends on the state under consideration. However, by bounding the variance (9) from above we can consider a worst-case scenario and determine the required values of M and K in order to reach a precision of at least δ with confidence γ (see App. II B). To do so, we use in the following the conjecture that the maximum of the fourth moment $\mathcal{R}^{(4)}$, for $N > 4$, is attained by the N -qubit GHZ states. While this assumption is backed by numerical evidence we leave its proof for future investigations.

In Fig. 3(left) we present the scaling of the required number of random measurement bases M with the number of subsystems N for different values of K . First, we note that the present statistical treatment allows for an improvement over the 3^N measurement settings that are required in order to evaluate the second moment exactly using a quantum design [17–20], at the expense of a non-zero statistical error from the unitary sampling. Second, the required number of random measurement settings M depends strongly on the chosen number of

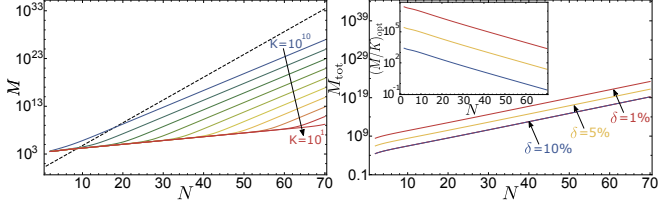


FIG. 3. Left: Required number M of sampled measurement bases in order to estimate $\mathcal{R}^{(2)}$ with an accuracy of at least 10% and confidence $\gamma = 90\%$ as a function of the number of subsystems N for $K = 10, 10^2, \dots, 10^{10}$ (solid curves from top to bottom) projective measurements. The black dashed line indicates the required measurement settings in order to exactly determine $\mathcal{R}^{(2)}$. Right: Total measurement budget $M_{\text{tot}}^{(\text{opt})} = M(K^{(\text{opt})}) \times K^{(\text{opt})}$ required for an estimation of $\mathcal{R}^{(2)}$ with accuracy 10% (bottom blue curve), 5% (middle yellow curve), and 1% (top red curve) as a function of N . Inset: Optimal ratio (M/K)^(opt) for the accuracies 10% (bottom blue curve), 5% (middle yellow curve), and 1% (top red curve) as a function of N .

projective measurements per random unitary. More precisely, the different curves in Fig. 3(left) scale as $\mathcal{O}(1.2^N)$ up to a certain threshold value that depends on the number K . After this threshold the scaling with the number of qubits increases to $\mathcal{O}(2.25^N)$.

The above discussion thus indicates that there is an optimal ratio between M and K , which determines the optimal measurement budget $M_{\text{tot}} = M \times K$. The latter can be obtained analytically (see App. II B) leading to the optimal value $M_{\text{tot}}^{(\text{opt})} = M(K^{(\text{opt})}) \times K^{(\text{opt})}$, presented in Fig. 3(right). We thus find that the total measurement budget follows an overall scaling law of approximately $\mathcal{O}(1.5^N)$. Furthermore, while the required measurement resources increase slightly with higher precision, i.e., smaller δ , the asymptotic scaling remains the same (see Fig. 3(right)).

Finite statistics entanglement characterization.— Further on, we investigate closer the characterization of multiparticle entanglement based on the criteria (3). To do so $\tilde{\mathcal{R}}^{(2)}$ has to exceed the respective k -separability bounds (3) by at least δ . Hence, if we chose the required measurements according to Fig. 3, we can confirm with confidence γ that the true value of $\mathcal{R}^{(2)}$ violates the respective bound as well. Even more, since we aim to exclude the hypothesis that the state is, e.g., k -separable, we can improve our procedure by invoking upper bounds on the variances (9) for k -separable states, respectively, instead of the overall upper bound used in Fig. 3.

In the following, we assume again the noisy GHZ state $\rho_{\text{GHZ}}^{(N)}(p)$ and determine the total number of measurements M_{tot} that is required in order to certify a violation of the entanglement criteria (3). We emphasize that in each case this involves an allocation of the optimal ratio M/K , and thus the optimal $M_{\text{tot}}^{(\text{opt})}$. First, in Fig. 4(top

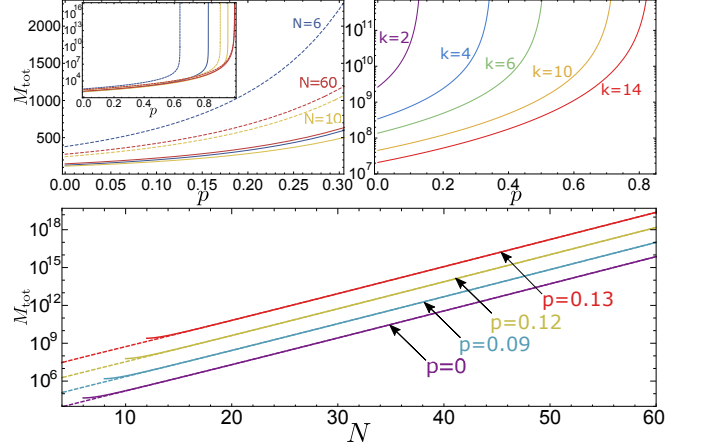


FIG. 4. Total measurement budget $M_{\text{tot}} = M(K_{\min})K_{\min}$ required to certify with a confidence of $\gamma = 90\%$ different types of multiparticle entanglement of the noisy GHZ state $\rho_{\text{GHZ}}^{(N)}(p)$. Top left: M_{tot} required to certify that $\rho_{\text{GHZ}}^{(N)}(p)$ is entangled (solid lines) or not in the W -class (dashed lines) for $N = 6$ (blue), $N = 10$ (yellow), and $N = 60$ (red) qubits as a function of the parameter p in the range $0 \leq p \leq 0.3$. The inset shows an extended plot in the range $0 \leq p \leq 1$. Top right: M_{tot} required to certify that the same state violates the k -separability criteria (3), with $k = 2$ (violet, left), 4 (blue), 6 (green), 10 (yellow) and 14 (red, right), for $N = 30$ qubits as a function of p . Bottom: M_{tot} required to certify GME for $p = 0$ (violet, bottom), $p = 0.09$ (cyan) $p = 0.12$ (yellow) and $p = 0.13$ (red, top) as a function of the number of qubits N . Solid and dashed lines refer to the cases of even and odd N , respectively.

left) we consider two known criteria allowing to detect states which are not fully-separable or not in the class of W -type entangled states [17–20]. We find that already moderate numbers of less than $M_{\text{tot}} = 2000$ are enough to certify their violation for up to $N = 60$ qubits. Divergences displayed in Fig. 4 are generally due to the asymptotically decreasing difference between the true value of $\mathcal{R}^{(2)}$ of the state under consideration and the respective bound of the targeted criterion. A similar behavior can be observed for the violation of different degrees of k -separability (see Fig. 4(top right)). In this case M_{tot} is generally on a higher level due to the increasing tightness of the bounds (3) for smaller k . Lastly, in Fig. 4(bottom) we focus on the detection of GME as a function of N . We find that the overall scaling of measurement in order to prove GME of $\rho_{\text{GHZ}}^{(N)}(p)$ follows approximately the law $\mathcal{O}(1.62^N)$, regardless of the precise choice of p .

Experimental implications.— Lastly, in order to demonstrate the applicability of our framework, we refer to recent experiments producing GHZ states with limited fidelity [32–34, 45]. For instance, in Ref. [32] a GHZ state of 11 qubits was produced with fidelity $F \approx 0.75$. By applying our formalism we can thus show that the state contains at least 5- or 7-particle entanglement by

performing in total of the order of 10^5 or 10^6 measurements, respectively (see App. II C for the precise numbers). Note that these numbers are still moderate in comparison to performing a full state tomography. Furthermore, we can show that the 20 qubit GHZ state of fidelity $F \approx 0.44$ (see Ref. [32]) contains at least 4- or 5-particle entanglement by performing in total of the order of 10^7 measurements. We emphasize that such insights cannot be reached in terms of the fidelity, since fidelities up to $1/2$ can be reproduced by fully separable states.

Conclusions.— We have discussed a statistical approach for the characterization of multiparticle quantum systems based on moments of correlation functions obtained from locally randomized measurements. In particular, we introduced novel criteria for the characterization of different classes of multiparticle correlations of N qubit systems, including genuine multiparticle entanglement, based on the lowest non-vanishing moment. Furthermore, a statistical analysis was carried out with the goal to determine the total number of measurements that is required in order to obtain estimates of the consid-

ered quantities with a well-defined error and confidence. Lastly, we applied to the developed statistical methods in order to certify different types of multiparticle entanglement based on finite statistics.

Our results are reminiscent of similar protocols based on so-called classical shadows which have proven useful for the evaluation of linear [14] and nonlinear [29] properties of the underlying quantum state. Hence, they further demonstrate the potential of protocols based on randomized measurements for the characterization of multiparticle quantum systems, in particular, in the noisy intermediate regime.

We thank Lukas Knips for discussions. This work was supported by the Deutsche Forschungsgemeinschaft (DFG, German Research Foundation) - Projektnummern 447948357 and 440958198, and the ERC (Consolidator Grant 683107/TempoQ). AK acknowledges support by the Georg H. Endress foundation. NW acknowledges support by the QuantERA grant QuICHE and the German ministry of education and research (BMBF, grant no. 16KIS1119K).

APPENDIX

I. MOMENTS OF RANDOM CORRELATIONS.

A. Definition of moments

For completeness we repeat below the main definitions presented at the beginning of the main text. There we characterized a random measurement through a set of random bases $\{(|u_n^{(0)}\rangle = U_n|0_n\rangle, |u_n^{(1)}\rangle = U_n|1_n\rangle)\}_{n=1,\dots,N}$, with $\{U_n\}_{n=1,\dots,N}$ picked from the unitary group $\mathcal{U}(2)$ according to the Haar measure μ . Further on, we associate to each element $(|u_n^{(0)}\rangle = U_n|0_n\rangle, |u_n^{(1)}\rangle = U_n|1_n\rangle)$, with $n \in \{1, \dots, N\}$, a direction \mathbf{u}_n on the unit sphere S^2 with components $[\mathbf{u}_n]_i = \text{tr}[\sigma_{\mathbf{u}_n} \sigma_i]$, with $i \in \{x, y, z\}$, and $\sigma_{\mathbf{u}_n} = U_n \sigma_z U_n^\dagger$ (see Fig. 1(a) of the main text). One such random measurement then enables us to retrieve the correlation functions:

$$E^{(\alpha_1, \dots, \alpha_{N'})}(\mathbf{u}_1, \dots, \mathbf{u}_{N'}) = \langle \sigma_{\mathbf{u}_1}^{(\alpha_1)} \dots \sigma_{\mathbf{u}_{N'}}^{(\alpha_{N'})} \rangle_\rho. \quad (10)$$

where $\sigma_{\mathbf{u}_j}^{(\alpha_j)}$ denotes the Pauli matrix $\sigma_{\mathbf{u}_j}$ with support on the α_j -th qubit, with $\alpha_j \in \{1, \dots, N'\}$ and $N' \leq N$.

The correlation functions (10) provide a random snapshot of the correlation properties of the output state ρ . In order to get a more complete picture one has to consider the corresponding moments

$$\mathcal{R}_{(\alpha_1, \dots, \alpha_{N'})}^{(t)} = \frac{1}{(4\pi)^{N'}} \int_{S^2} d\mathbf{u}_1 \dots \int_{S^2} d\mathbf{u}_{N'} \left[E^{(\alpha_1, \dots, \alpha_{N'})}(\mathbf{u}_1, \dots, \mathbf{u}_{N'}) \right]^t, \quad (11)$$

where t is a positive integer and $d\mathbf{u}_i = \sin\theta_i d\theta_i d\phi_i$ the uniform measure on the sphere S^2 . Note that in the main text we focus solely on moments evaluated with full-correlation functions, i.e., correlation functions over all N subsystems. In this case we drop the subscripts $(\alpha_1, \dots, \alpha_{N'})$ and refer to it as the respective N -qubit moment. As mentioned previously the moments (11) are by definition invariant under local unitary transformation, i.e., LU-invariant. Furthermore, due to the symmetries of the correlation functions (10) with respect to a reflection on the local Bloch spheres, e.g. $E(\mathbf{u}_1, \dots, -\mathbf{u}_i, \dots, \mathbf{u}_N) = -E(\mathbf{u}_1, \dots, \mathbf{u}_N)$, it is easy to see that all odd moments will vanish. We note that this is no longer true if one considers moments of quantum systems with larger local dimensionality [20].

In the following we will focus on the N -qubit moments and discuss several important properties. Eventually, we prove a criterion for the detection of genuine multipartite entanglement (GME) based on the second moment only.

B. Moments and spherical designs

In Refs. [19, 20] it was discussed that the integrals involved in the moments $\mathcal{R}^{(t)}$ can be replaced by an appropriate sum whenever an appropriate spherical t -design is known. In general, a spherical t -design in dimension three consist of a finite set of points $\{\mathbf{u}_i | i = 1, \dots, L^{(t)}\} \subset S^2$ fulfilling the property

$$\frac{1}{L^{(t)}} \sum_{k=1}^{L^{(t)}} P_{t'}(\mathbf{u}_k) = \frac{1}{4\pi} \int_{S^2} d\mathbf{u} P_{t'}(\mathbf{u}), \quad (12)$$

for all homogeneous polynomials $P_{t'} : S^2 \rightarrow \mathbb{R}$, with $t' \leq t$. It thus suffices to resort to spherical t -designs as long as one is interested in calculating averages of polynomials of degree at most t over the Bloch sphere S^2 . This leads to the expression

$$\mathcal{R}^{(t)} = \frac{1}{(L^{(t)})^N} \sum_{k_1, \dots, k_N=1}^{L^{(t)}} \langle \sigma_{\mathbf{u}_{k_1}} \otimes \dots \otimes \sigma_{\mathbf{u}_{k_N}} \rangle^t. \quad (13)$$

Specifically, several concrete spherical designs on the 2-sphere S^2 for t 's up to 20 and consisting of up to 100 elements are known (see for instance Ref. [46]). See Fig. 2 of Ref. [47] for examples. Using these spherical designs the second moment can be expressed as follows

$$\mathcal{R}^{(2)} = \frac{1}{3^N} \sum_{i_1, \dots, i_N=x,y,z} E(\mathbf{e}_{i_1}, \dots, \mathbf{e}_{i_N})^2, \quad (14)$$

by summing over the three Pauli observables only. For higher order moments we need higher order designs, respectively. For instance, the fourth moment becomes

$$\mathcal{R}^{(4)} = \frac{1}{6^N} \sum_{i_1, \dots, i_N=1}^6 E(\mathbf{v}_{i_1}, \dots, \mathbf{v}_{i_N})^4, \quad (15)$$

where the $\{\mathbf{v}_i | i = 1, \dots, L^{(5)} = 12\}$ denotes the icosahedron 5-design discussed in Ref. [47]. Note that in Eq. (14) and (15) the number of summands is $L^{(t)}/2$ because for even t one can drop the anti-parallel settings $-\mathbf{e}_i$ and $-\mathbf{v}_i$, respectively.

C. Bounds of the moments $\mathcal{R}^{(2)}$ and $\mathcal{R}^{(4)}$

Generally the moments (11) are upper and lower bounded depending on the class of quantum states under consideration. Furthermore, these bounds are in most cases dependent on the number of subsystems they are evaluated on. In this section we will summarize some known bounds thus yielding the basis for the novel GME-criterion introduced later on.

First, we consider the class $\mathcal{B}((\mathbb{C}^2)^{\otimes N})$ of all mixed N -qubit quantum states. In this case all moments $\mathcal{R}^{(t)}$ are bounded from below by zero and equality is reached for the maximally mixed state. This is easy to see as all odd moments are zero and all even moments are positive. In contrast, it is much more difficult to determine tight upper bounds of the moments. Even only for the second moment $\mathcal{R}^{(2)}$ this problem has been solved only recently. In Refs. [18, 42, 43] it was shown that the maximum value of the second moment is reached for the N -qubit GHZ state $|\text{GHZ}_N\rangle = (|0\rangle^{\otimes N} + |1\rangle^{\otimes N})/\sqrt{2}$, yielding

$$\mathcal{R}_{|\text{GHZ}_N\rangle}^{(2)} = \frac{1}{3^N} \times \begin{cases} 2^{N-1}, & N \text{ odd}, \\ 2^{N-1} + 1, & N \text{ even}. \end{cases} \quad (16)$$

This insight was derived through the relation of the second moment to so-called sector lengths. The N -sector length is basically equal to Eq. (14) if one omits the proportionality factor of $1/3^N$. Upper bounds of higher moments are unfortunately not known in general. However, we have numerical evidence that the upper bound of the fourth moment $\mathcal{R}^{(4)}$ is also reached for the GHZ state for which we find the values

$$\mathcal{R}_{|\text{GHZ}_N\rangle}^{(4)} = \frac{1}{15^N} \begin{cases} 3 \times 8^{N-1}, & N \text{ odd}, \\ 3 \times 8^{N-1} + 3^N + 3 \times 2^N, & N \text{ even}. \end{cases} \quad (17)$$

We did not find a state that has a larger fourth moment than the one of Eq. (17) except for the special case $N = 4$. In this case the bi-separable state $|\text{Bell}\rangle \otimes |\text{Bell}\rangle$ reaches a larger value than the GHZ state. However, for an $N/2$ -fold product of Bell states $|\text{Bell}\rangle^{\otimes(N/2)}$, with N even, the fourth moment reads

$$\mathcal{R}_{|\text{Bell}\rangle^{\otimes\frac{N}{2}}}^{(4)} = \frac{1}{5^{(N/2)}}. \quad (18)$$

Also, other product states like $|\text{GHZ}_{\frac{N}{2}}\rangle \otimes |\text{GHZ}_{\frac{N}{2}}\rangle$ have a smaller fourth moment than Eq. (17), which is easy to check as the moments $\mathcal{R}^{(t)}$ factorize for product states.

Second, if we consider the class of separable states $\rho_{\text{sep}} = \sum_{\alpha} p_{\alpha} \rho_{\alpha}^{(1)} \otimes \dots \otimes \rho_{\alpha}^{(N)}$ we can also derive upper bounds on the moments [19]. To do so, we simply exploit the convexity of the even moments which relies on the convexity of the monomials x^t for even t . Furthermore, we know that for $N = 1$ we find for all pure states $\mathcal{R}_{N=1}^{(2)} = \frac{1}{3}$ and $\mathcal{R}_{N=1}^{(4)} = \frac{1}{5}$. Hence, all in all we find the following bounds

$$\mathcal{R}^{(2)} \leq 1/3^N, \quad \mathcal{R}^{(4)} \leq 1/5^N, \quad (19)$$

for all separable N -qubit states ρ_{sep} .

Lastly, it has also been shown that one can derive upper bounds on the moments for different multipartite entanglement classes. For instance, in Ref. [20] it was reported that the second moment is bounded from above by

$$\mathcal{R}^{(2)} \leq \frac{5 - \frac{4}{N}}{3^N} =: \chi^{(N)}, \quad (20)$$

for all states contained in the mixed N -qubit W -class. The latter is defined as $\text{Conv}(\mathcal{W}^{(N)})$, where $\text{Conv}(\dots)$ denotes the convex hull and $\mathcal{W}^{(N)}$ the pure N -qubit SLOCC (stochastic local operations and classical communication) class.

D. Multiparticle entanglement criteria

In this section we prove the criteria introduced in Eq. (3) of the main text. We start with the case $k = 2$, i.e., the criterion allowing to detect genuinely multipartite entanglement. To do so, let us first consider a pure biseparable state of N -qubits

$$\rho_{\text{bisep}} = \rho_{N-k} \otimes \rho_k \quad (21)$$

with $k \in \{1, \dots, N/2\}$, and calculate the maximum of its second moment

$$\begin{aligned} \max_{\rho_{\text{bisep}}} \mathcal{R}_{\rho_{\text{bisep}}}^{(2)} &= \max_k \mathcal{R}_{\rho_{N-k}}^{(2)} \times \max_k \mathcal{R}_{\rho_k}^{(2)} \\ &= \frac{1}{3^N} \begin{cases} 2^{N-k-1}, & N-k \text{ odd} \\ 2^{N-k-1} + 1, & N-k \text{ even} \end{cases} \times \begin{cases} 2^{k-1}, & k \text{ odd} \\ 2^{k-1} + 1, & k \text{ even} \end{cases}, \end{aligned} \quad (22)$$

where we used that the maximum of an m -qubit second moment is attained for the respective m -qubit GHZ state (see Eq. (16)). Further on, if N is assumed to be even we find

$$\begin{aligned} \max_{\rho_{\text{bisep}}} \mathcal{R}_{\rho_{\text{bisep}}}^{(2)} &= \frac{1}{3^N} \max_k \begin{cases} 2^{N-k-1} \times 2^{k-1}, & k \text{ odd} \\ (2^{N-k-1} + 1) \times (2^{k-1} + 1), & k \text{ even} \end{cases} \\ &= \frac{1}{3^N} \max_k \begin{cases} 2^{N-2}, & k \text{ odd} \\ 2^{N-2} + 2^{N-k-1} + 2^{k-1} + 1, & k \text{ even} \end{cases} \end{aligned} \quad (23)$$

$$= \frac{1}{3^N} \left[2^{N-2} + 1 + \max_k (2^{N-k-1} + 2^{k-1}) \right] \quad (24)$$

$$= \frac{2^{N-3} + 1}{3^{N-1}}, \quad (25)$$

where we used that the function $f(k) = 2^{N-k-1} + 2^{k-1}$ is positive on the interval $[2, N-2]$ and thus takes its maximum at the boundary, i.e., for $k = 2$ or $k = N-2$. Instead, if N is odd we find

$$\begin{aligned} \max_{\rho_{\text{bise}}}\mathcal{R}_{\rho_{\text{bise}}}^{(2)} &= \frac{1}{3^N} \max_k \begin{cases} (2^{N-k-1} + 1) \times 2^{k-1}, & k \text{ odd} \\ 2^{N-k-1} \times (2^{k-1} + 1), & k \text{ even} \end{cases} \\ &= \frac{1}{3^N} \max_k \begin{cases} 2^{N-2} + 2^{k-1}, & k \text{ odd} \\ 2^{N-2} + 2^{N-k-1}, & k \text{ even} \end{cases} \end{aligned} \quad (26)$$

$$= \frac{1}{3^N} \left[2^{N-2} + \max_k \begin{cases} 2^{k-1}, & k \text{ odd} \\ 2^{N-k-1}, & k \text{ even} \end{cases} \right] \quad (27)$$

$$= \frac{1}{3^N} \left[2^{N-2} + \max_k (2^{N-k-1}) \right] = \frac{2^{N-3}}{3^{N-1}}, \quad (28)$$

where we used that $g(k) = 2^{N-k-1}$ is positive in the interval $[2, N/2]$ and its maximum is reached for $k = 2$. In summary, we thus proved that

$$\mathcal{R}^{(2)} \leq \frac{1}{3^{N-1}} \times \begin{cases} 2^{N-3}, & N \text{ odd}, \\ 2^{N-3} + 1, & N \text{ even}. \end{cases} \quad (29)$$

for all biseparable states ρ_{bise} . If we compare the bound (29) with the maximum value of the second moment (16) we find that for odd number of qubits $2^{N-1}/3^N > 2^{N-3}/3^{N-1}$, for all N . For even number of qubits we have $(2^{N-1} + 1)/3^N \geq (2^{N-3} + 1)/3^{N-1}$, for all N , with equality iff $N = 4$. Hence, the N -qubit second moment allows for the detection of genuine multipartite entanglement as long as $N \neq 4$. Furthermore, we note that the bounds in Eq. (29) are saturated for the states $|\text{Bell}\rangle \otimes |\text{GHZ}_{(N-2)}\rangle$.

Further on, we show that for k -separable states $\mathcal{R}^{(2)}$ obeys the bounds

$$\mathcal{R}^{(2)} \leq \frac{1}{3^{N-k+1}} \times \begin{cases} 2^{N-(2k-1)}, & N \text{ odd}, \\ 2^{N-(2k-1)} + 1, & N \text{ even}, \end{cases} \quad (30)$$

with $k = 2, \dots, \lfloor (N-1)/2 \rfloor$, a prove of which can be carried through the method of induction. Since we have proven Eq. (30) in the case $k = 2$, it remains the induction step, i.e., that the case $k+1$ follows from k . First, assume that N is even and that for a k -separable state of $N-m$ qubits, denoted as ρ_{N-m} , the following holds

$$\mathcal{R}_{\rho_{N-m}}^{(2)} \leq \frac{1}{3^{N-m-k+1}} \times \begin{cases} 2^{N-m-(2k-1)}, & N-m \text{ odd}, \\ 2^{N-m-(2k-1)} + 1, & N-m \text{ even}. \end{cases} \quad (31)$$

Now, we consider the maximum of the second moment of an N -qubit $(k+1)$ -separable state

$$\max_{\rho_{(k+1)\text{-sep}}}\mathcal{R}_{\rho_{(k+1)\text{-sep}}}^{(2)} = \max_m \mathcal{R}_{\rho_{k\text{-sep},N-m}}^{(2)} \times \max_m \mathcal{R}_{\rho_m}^{(2)} \quad (32)$$

where $\rho_{k\text{-sep},x}$ denotes a k -separable state of x qubits. Further on, we know by assumption that

$$\mathcal{R}_{\rho_{k\text{-sep},N-m}}^{(2)} \leq \frac{1}{3^{N-m-k+1}} (2^{N-m-(2k-1)} + \delta_{(N-m),\text{even}}) \quad (33)$$

and, according to Eq. (16), that

$$\mathcal{R}_{\rho_m}^{(2)} \leq \frac{1}{3^m} (2^{m-1} + \delta_{m,\text{even}}). \quad (34)$$

Consequently, the RHS of Eq. (32) becomes

$$\max_{\rho_{(k+1)\text{-sep}}}\mathcal{R}_{\rho_{(k+1)\text{-sep}}}^{(2)} = \max_m \left\{ \frac{1}{3^{N-m-k+1}} \times (2^{N-m-(2k-1)} + \delta_{(N-m),\text{even}}) \times \frac{1}{3^m} (2^{m-1} + \delta_{m,\text{even}}) \right\} \quad (35)$$

which takes its maximum for even m and thus leads to

$$\max_{\rho_{(k+1)\text{-sep}}} \mathcal{R}_{\rho_{(k+1)\text{-sep}}}^{(2)} = \frac{1}{3^{N-k+1}} \times \max_m \{(2^{N-m-(2k-1)} + 1) \times (2^{m-1} + 1)\} \quad (36)$$

$$= \frac{1}{3^{N-k+1}} \times \max_m \{(2^{N-2k} + 2^{N-m-(2k-1)} + 2^{m-1} + 1)\}, \quad (37)$$

where in the last two lines we assumed that m is even. It thus remains to maximize Eq. (37) with respect to m . The m -dependent terms of Eq. (37) can be written as $g(M) = \frac{2^{N+1-2k}}{M} + \frac{M}{2}$, with $M := 2^m$, which is convex and thus attains its maximum at the boundary $M = 2^m = 2^2$, and thus for $m = 2$. Altogether this leads to

$$\mathcal{R}^{(2)} \leq \frac{2^{N-(2k-1)}}{3^{N-k+1}}, \quad (38)$$

for even N . An analogous calculation can be carried out for odd N . We note that the respective k -separability bounds (30) are attained by the following class of pure k -separable states $|\text{Bell}\rangle^{\otimes(k-1)} \otimes |\text{GHZ}_{N-2(k-1)}\rangle$, which can be verified easily by explicitly evaluating the corresponding moment $\mathcal{R}^{(2)}$ for the respective states.

Similarly, we can formulate k -separable bounds of the fourth moment $\mathcal{R}^{(4)}$ which plays an important role for the determination of the measurement resources required in order to violate Eq. (30) with a given confidence. Based on the conjecture that for $N > 4$ the N -qubit GHZ state maximizes the fourth moment $\mathcal{R}^{(4)}$ we can show that

$$\mathcal{R}^{(4)} \leq \frac{1}{5^{k-1}} \mathcal{R}_{|\text{GHZ}_{N-2(k-1)}\rangle}^{(4)}, \quad (39)$$

using similar methods as in the proof of Eq. (30). As for the second moment $\mathcal{R}^{(2)}$, the bound in Eq. (39) is saturated for the k -separable pure states $|\text{Bell}\rangle^{\otimes(k-1)} \otimes |\text{GHZ}_{N-2(k-1)}\rangle$, with $k = 2, \dots, \lfloor (N-1)/2 \rfloor$.

E. Entanglement depth

Instead of bounding the moments $\mathcal{R}^{(t)}$ for k -separable states, one can derive bounds for the class of so-called m -producible states. The latter are characterized by the fact that they contain at least m -particle entanglement. More precisely, a pure state $|\Psi\rangle$ of N particles is called producible by m -particle entanglement, i.e., m -producible, if it can be written as

$$|\Psi\rangle = |\phi_1\rangle \otimes |\phi_2\rangle \otimes \dots \otimes |\phi_\ell\rangle \quad (40)$$

where $|\phi_i\rangle$ are states of maximally m particles and $\ell \geq N/m$. Hence, a state is called genuinely m -particle entangled if it is not producible by $(m-1)$ -particle entanglement and thus has an entanglement depth of m . As for k -separable states, the above definition can be extended to mixed states by allowing for convex combinations of m -separable states.

Based on the above definition we can proceed and derive bounds on the second moment $\mathcal{R}^{(2)}$ for m -producible states. To do so, we assume a pure m -separable states $|\Psi_m\rangle = |\phi_1\rangle \otimes |\phi_2\rangle \otimes \dots \otimes |\phi_\ell\rangle$, where $|\phi_j\rangle$ consists of m_j particles, for which we obtain

$$\mathcal{R}_{|\Psi_m\rangle}^{(2)} = \mathcal{R}_{|\phi_1\rangle}^{(2)} \times \mathcal{R}_{|\phi_2\rangle}^{(2)} \times \dots \times \mathcal{R}_{|\phi_\ell\rangle}^{(2)} \quad (43)$$

$$\leq \mathcal{R}_{|\text{GHZ}_{m_1}\rangle}^{(2)} \times \mathcal{R}_{|\text{GHZ}_{m_2}\rangle}^{(2)} \times \dots \times \mathcal{R}_{|\text{GHZ}_{m_\ell}\rangle}^{(2)} \quad (44)$$

where we used that each $\mathcal{R}_{|\phi_j\rangle}^{(2)}$ is maximized by the respective m_j -qubit GHZ state. In order to maximize the RHS of Eq. (44) we have to go simply through all possible assignments of m_j 's such that their sum equals to N . By rearranging terms we thus find:

$$\mathcal{R}_{|\Psi_m\rangle}^{(2)} \leq \left(\mathcal{R}_{|\text{GHZ}_1\rangle}^{(2)} \right)^{k_1} \left(\mathcal{R}_{|\text{GHZ}_2\rangle}^{(2)} \right)^{k_2} \times \dots \times \left(\mathcal{R}_{|\text{GHZ}_m\rangle}^{(2)} \right)^{k_m} \quad (45)$$

with $\sum_{i=1}^m ik_i = N$, and where $|\text{GHZ}_1\rangle$ and $|\text{GHZ}_2\rangle$ refer to a single qubit pure state and one of the Bell states, respectively. Finding the maximum of the RHS of Eq. (45) for a given N is thus a simple task. In Table I we give the m -producibility bounds of $\mathcal{R}^{(2)}$ for $N = 11$ and $N = 20$. Indeed, we find that for larger m 's the bounds often coincide with the k -separability bounds given in Eq. (30), but can in general also differ from. While it might be possible to derive a general and concise formula, as for k -separable states (see Eq. (30)), we leave this task for future investigations.

$N = 11$:

m	$\mathcal{R}_{m-\text{prod.}}^{(2)}$	(k_1, k_2, \dots, k_m)
2	$\frac{1}{729}$	$(k_1 = 1, k_2 = 5)$
3	$\frac{4}{2187}$	$(k_1 = 0, k_2 = 4, k_3 = 1)$
4	$\frac{4}{2187}$	$(k_1 = 0, k_2 = 0, k_3 = 1, k_4 = 2)$
5	$\frac{16}{6561}$	$(k_1 = 0, k_2 = 1, k_3 = 0, k_4 = 1, k_5 = 1)$
6	$\frac{176}{59049}$	$(k_1 = 0, k_2 = 0, k_3 = 0, k_4 = 0, k_5 = 1, k_6 = 1)$
7	$\frac{64}{19683}$	$(k_1 = 0, k_2 = 0, k_3 = 0, k_4 = 1, k_5 = 0, k_6 = 0, k_7 = 1)$
8	$\frac{64}{19683}$	$(k_1 = 0, k_2 = 0, k_3 = 0, k_4 = 1, k_5 = 0, k_6 = 0, k_7 = 1, k_8 = 0)$
9	$\frac{256}{59049}$	$(k_1 = 0, k_2 = 1, k_3 = 0, k_4 = 0, k_5 = 0, k_6 = 0, k_7 = 0, k_8 = 0, k_9 = 1)$
10	$\frac{256}{59049}$	$(k_1 = 0, k_2 = 1, k_3 = 0, k_4 = 0, k_5 = 0, k_6 = 0, k_7 = 0, k_8 = 0, k_9 = 1, k_{10} = 0)$

$N = 20$:

m	$\mathcal{R}_{m-\text{prod.}}^{(2)}$	(k_1, k_2, \dots, k_m)
2	$\frac{1}{59049}$	$(k_1 = 0, k_2 = 10)$
3	$\frac{1}{59049}$	$(k_1 = 0, k_2 = 10, k_3 = 0)$
4	$\frac{1}{59049}$	$(k_1 = 0, k_2 = 0, k_3 = 0, k_4 = 5)$
5	$\frac{65536}{3486784401}$	$(k_1 = 0, k_2 = 0, k_3 = 0, k_4 = 0, k_5 = 4)$
6	$\frac{65536}{3486784401}$	$(k_1 = 0, k_2 = 1, k_3 = 0, k_4 = 0, k_5 = 0, k_6 = 3)$
7	$\frac{45056}{1162261467}$	$(k_1 = 0, k_2 = 0, k_3 = 0, k_4 = 0, k_5 = 0, k_6 = 1, k_7 = 2)$
8	$\frac{1849}{43046721}$	$(k_1 = 0, k_2 = 0, k_3 = 0, k_4 = 1, k_5 = 0, k_6 = 0, k_7 = 0, k_8 = 2)$
9	$\frac{65536}{1162261467}$	$(k_1 = 0, k_2 = 1, k_3 = 0, k_4 = 0, k_5 = 0, k_6 = 0, k_7 = 0, k_8 = 0, k_9 = 2)$
10	$\frac{361}{4782969}$	$(k_1 = 0, k_2 = 0, k_3 = 0, k_4 = 0, k_5 = 0, k_6 = 0, k_7 = 0, k_8 = 0, k_9 = 0, k_{10} = 2)$

TABLE I. Numerical values of the m -producibility bounds, with $m = 2, \dots, 10$, and the respective assignments (k_1, k_2, \dots, k_m) (see Eq. (45)) of the second moment $\mathcal{R}^{(2)}$ for 11 (upper table) and 20 (lower table) qubits.

II. ESTIMATION OF MOMENTS WITH FINITE STATISTICS

A. Unbiased estimators and their variance

As explained in the main text we denote individual outcomes of a single random measurement on N qubits by $\{r_1, \dots, r_N\}$, with $r_i = \pm 1$, and the corresponding correlation sample as $X = \prod_{i=1}^N r_i$ (see Fig. 1(a) of the main text). Similarly, the correlation samples of subsets of N' qubits are obtained by focusing on the respective outcomes $\{r_1^{(\alpha_1)}, \dots, r_{N'}^{(\alpha_{N'})}\}$. Next, we define the probability P for obtaining the result $X = +1$, i.e., if an even number of the individual measurement outcomes r_i resulted in -1 . The corresponding unbiased estimator of P can be defined as follows $\tilde{P}_1 := Y/K$, where Y is a random variable distributed according to the binomial distribution with probability P and K trials. We thus find $\mathbb{E}_{\text{bi}}(\tilde{P}_1) = P$, where $\mathbb{E}_{\text{bi}}(\dots)$ denotes the average with respect to the binomial distribution. We note that similar methods have been employed also in Ref. [23] in the context of globally randomized measurement protocols.

Similarly, we can define unbiased estimator \tilde{P}_k for the k -th powers of P by making the ansatz $\tilde{P}_k = \sum_{i=0}^k \alpha_i (\tilde{Y}/K)^i$ and enforcing the relation $\mathbb{E}(\tilde{P}_k) = P^k$. Hence, by using only the properties of the binomial distribution we can define unbiased estimators for arbitrary powers of P . For instance, we find

$$\tilde{P}_2 = \frac{\tilde{P}_1(K\tilde{P}_1 - 1)}{K-1} = \tilde{P}_1 \times \frac{K\tilde{P}_1 - 1}{K-1}, \quad (46)$$

$$\tilde{P}_3 = \frac{\tilde{P}_1(K\tilde{P}_1 - 1)(K\tilde{P}_1 - 2)}{(K-1)(K-2)} = \tilde{P}_2 \times \frac{K\tilde{P}_1 - 2}{K-2}, \quad (47)$$

$$\tilde{P}_4 = \frac{\tilde{P}_1(K\tilde{P}_1 - 1)(K\tilde{P}_1 - 2)(K\tilde{P}_1 - 3)}{(K-1)(K-2)(K-3)} = \tilde{P}_3 \times \frac{K\tilde{P}_1 - 3}{K-3}, \quad (48)$$

which leads recursively to the following estimator for the t -th moment

$$\tilde{P}_k = \tilde{P}_{k-1} \times \frac{K\tilde{P}_1 - (k-1)}{K - (k-1)} = \frac{\tilde{P}_1(K\tilde{P}_1 - 1)(K\tilde{P}_1 - 2) \dots (K\tilde{P}_1 - (k-1))}{(K-1)(K-2) \dots (K-(k-1))}. \quad (49)$$

Equation (49) can be easily verified to be the unbiased estimator of P^k by noting that the factorial moment of the binomial distribution reads $\mathbb{E}_{\text{bi}}[Y(Y-1)\dots(Y-(k-1))] = K!P^t/(k-t)!$ [48]. Further on, the unbiased estimators of the t -th powers of the correlations functions $E = 2P - 1$ can be obtained straightforwardly with formula

$$\tilde{E}_t = (-1)^t \sum_{k=0}^t (-2)^k \binom{t}{k} \tilde{P}_k = (-1)^t \sum_{k=0}^t (-2)^k \binom{t}{k} \left[\frac{\tilde{P}_1(K\tilde{P}_1-1)(K\tilde{P}_1-2)\dots(K\tilde{P}_1-(k-1))}{(K-1)(K-2)\dots(K-(k-1))} \right], \quad (50)$$

which, in turn, allows us to define faithful estimators of the corresponding moments (11):

$$\tilde{\mathcal{R}}^{(t)} = \frac{1}{M} \sum_{i=1}^M [\tilde{E}_t]_i. \quad (51)$$

We note that the subscript i refers to estimations of \tilde{E}_t for different randomly sampled local bases, thus making the $[\tilde{E}_t]_i$ i.i.d. random variables. That is, we have $\mathbb{E}_U \mathbb{E}_{\text{bi}}[(\tilde{\mathcal{R}}^{(t)})] = \mathcal{R}^{(t)}$, where $\mathbb{E}_U[\dots]$ denotes the average over local random unitaries. We thus have provided a toolbox allowing for a statistical evaluation of the moment $\mathcal{R}^{(t)}$. In order to estimate the statistical errors of these evaluations we have to regard the variance of the respective unbiased estimators (51), that is

$$\text{Var}(\tilde{\mathcal{R}}^{(t)}) = \mathbb{E}_U \mathbb{E}_{\text{bi}}[(\tilde{\mathcal{R}}^{(t)} - \mathcal{R}^{(t)})^2] = \mathbb{E}_U \mathbb{E}_{\text{bi}}[(\tilde{\mathcal{R}}^{(t)})^2] - (\mathcal{R}^{(t)})^2, \quad (52)$$

or by using Eq. (51)

$$\text{Var}(\tilde{\mathcal{R}}^{(t)}) = \frac{1}{M^2} \sum_{i=1}^M \text{Var}([\tilde{E}_t]_i), \quad (53)$$

since the $[\tilde{E}_t]_i$ are i.i.d. random variables. Hence, it suffices to evaluate the variance

$$\text{Var}([\tilde{E}_t]_i) = \mathbb{E}_U \mathbb{E}_{\text{bi}}[\tilde{E}_t^2] - (\mathbb{E}_U [\tilde{E}_t])^2 = \mathbb{E}_U \mathbb{E}_{\text{bi}}[\tilde{E}_t^2] - (\mathcal{R}^{(t)})^2. \quad (54)$$

where $\mathbb{E}_U \mathbb{E}_{\text{bi}}[\tilde{E}_t^2]$ is in general a function of the moments $\mathcal{R}^{(t)}$. For instance, if we focus on the particular case $t = 2$, we find

$$\text{Var}([\tilde{E}_2]_i) = A(K)\mathcal{R}^{(4)} + B(K)\mathcal{R}^{(2)} + C(K) - (\mathcal{R}^{(2)})^2, \quad (55)$$

with

$$A(K) := \frac{K}{K-1} - \frac{5}{K-1} + \frac{6}{(K-1)K}, \quad (56)$$

$$B(K) := \frac{4}{K-1} - \frac{8}{(K-1)K}, \quad (57)$$

$$C(K) := \frac{2}{K(K-1)}, \quad (58)$$

which leads to

$$\text{Var}(\tilde{\mathcal{R}}^{(2)}) = \frac{1}{M} \left[A(K)\mathcal{R}_{|\text{GHZ}_N\rangle}^{(4)} + B(K)\mathcal{R}_{|\text{GHZ}_N\rangle}^{(2)} + C(K) - (\mathcal{R}^{(2)})^2 \right]. \quad (59)$$

In order to arrive at the worst case error discussed in the main text we upper bound Eq. (59) by discarding the term $(\mathcal{R}^{(2)})^2$ and using Eqs. (16) and (17) which leads to

$$\begin{aligned} \text{Var}(\tilde{\mathcal{R}}^{(2)}) &\leq \frac{1}{M} \left[A(K)\mathcal{R}_{|\text{GHZ}_N\rangle}^{(4)} + B(K)\mathcal{R}_{|\text{GHZ}_N\rangle}^{(2)} + C(K) \right] \\ &= \frac{1}{M} \left[A(K) \begin{cases} 3 \times 8^{N-1}/15^N, & N \text{ odd,} \\ (3 \times 8^{N-1} + 3^N + 3 \times 2^N)/15^N, & N \text{ even.} \end{cases} \right. \\ &\quad \left. + B(K) \times \begin{cases} 2^{N-1}/3^N, & N \text{ odd,} \\ (2^{N-1} + 1)/3^N, & N \text{ even.} \end{cases} + C(K) \right]. \end{aligned} \quad (60)$$

Hence, we found a state independent upper bound of the error on the estimator $\tilde{\mathcal{R}}^{(2)}$ which still involves a dependence on the number of subsystems N . The latter is important because the maxima of the moments tend to decrease with increasing N .

B. Measurement resources for an estimation of $\mathcal{R}^{(2)}$

Using the variance bound derived in Eq. (60) we can now derive a lower bound on the number of measurements $M \times K$ that is required in order to estimate $\mathcal{R}^{(2)}$ with accuracy δ and confidence γ (see Fig. 2(a) of the main text). To do so, we first regard the two-sided Chebyshev-Cantelli inequality for the random variable $\tilde{\mathcal{R}}^{(t)}$ yielding

$$\text{Prob}[|\tilde{\mathcal{R}}^{(t)} - \mathcal{R}^{(t)}| \geq \delta] \leq \frac{2\text{Var}(\tilde{\mathcal{R}}^{(t)})}{\text{Var}(\tilde{\mathcal{R}}^{(t)}) + \delta^2}, \quad (61)$$

which, by requiring that the confidence $1 - \text{Prob}[|\tilde{\mathcal{R}}^{(t)} - \mathcal{R}^{(t)}| \geq \delta] \geq \gamma$ of this estimation is at least γ , allows us to derive the following bound on the error of the estimation

$$\delta \leq \sqrt{\frac{1+\gamma}{1-\gamma} \text{Var}(\tilde{\mathcal{R}}^{(t)})}. \quad (62)$$

Furthermore, for the estimation of the second moment we can impose the variance bound of Eq. (60), yielding

$$\delta \leq \sqrt{\frac{1+\gamma}{1-\gamma} \frac{1}{M} \left[A(K) \mathcal{R}_{|\text{GHZ}_N\rangle}^{(4)} + B(K) \mathcal{R}_{|\text{GHZ}_N\rangle}^{(2)} + C(K) \right]}. \quad (63)$$

Now, Eq. (63) allows us to derive the required numbers of measurements M and K in order to reach a given error δ . Since the size of the interval $[0, \mathcal{R}_{|\text{GHZ}_N\rangle}^{(2)}]$ depends on the number of subsystems N , we ask for a minimum relative error, i.e., a fraction of the length of the whole length interval. Hence, in order to achieve an estimation of the second moment with a relative error δ_{rel} and with a confidence γ we require at least the following number of random measurement settings

$$M(K) = \frac{\gamma+1}{\gamma-1} \frac{16 \cdot 3^N \left((K-2) \left(-(2^N+2) \right) - 3^N \right) - (K-3)(K-2) \left(\frac{3}{5} \right)^N \left(3 \cdot 2^{N+3} + 8 \cdot 3^N + 3 \cdot 8^N \right)}{2(K-1)K \left(2^N+2 \right)^2 \delta_{\text{rel}}^2}, \quad (64)$$

which is also presented in Fig. 1(a) of the main text. Furthermore, in order to determine the optimal number of projective measurements per random measurement setting we minimize Eq. (64) with respect to K and with fixed number of parties N . To do so, we fix the desired confidence to $\gamma = 90\%$ which leads to

$$K_{\text{opt}} = 1 + \sqrt{2} \sqrt{1 - \frac{8 \cdot 5^N (2^N - 3^N + 2)}{3 \cdot 2^{N+3} + 8 \cdot 3^N + 3 \cdot 8^N}}, \quad (65)$$

which interestingly does no longer depend on the size of the error δ_{rel} . In summary, Eqs. (64) and (65) fix the ratio between M and K and thus the total number of required measurement runs $M_{\text{tot}} = M \times K_{\text{opt}}$ as a function of the system size N (see Fig. 2(b) of the main text).

C. Characterizing the entanglement properties of the noisy GHZ state $\rho_{\text{GHZ}}^{(N)}(p)$

Using similar methods as in the previous section we can determine the measurement resources required for a detection of different degrees of multiparticle entanglement with confidence γ (see Fig. 4 of the main text). In this case we can resort to the one-sided Chebyshev-Cantelli inequality

$$\text{Prob}[\tilde{\mathcal{R}}^{(2)} - \mathcal{R}^{(2)} \geq \delta] \leq \frac{\text{Var}(\tilde{\mathcal{R}}^{(2)})}{\text{Var}(\tilde{\mathcal{R}}^{(2)}) + \delta^2}. \quad (66)$$

as we have to show only that $\mathcal{R}^{(2)}$ is larger than the given bounds of the criteria (30). Also, since we want to rule out the hypothesis that the state belongs to a certain class of separable states, we can invoke the respective upper bounds of the second and fourth moment in order to upper bound the variance $\text{Var}(\tilde{\mathcal{R}}^{(2)})$. In doing we further improve the required measurement resources in comparison to the overall worst-case scenario for an estimation of $\mathcal{R}^{(2)}$ considered in Sec. B.2.

For instance, for the detection of non- k -separability we use Eqs. (30) and (39) in order to upper bound the variance in Eq. (66). Furthermore, we set the confidence $\gamma = 90\%$ and the accuracy $\delta = \mathcal{R}_{\text{GHZ}}^{(2)}(p, N) - \max \mathcal{R}_{\rho_{k-\text{sep}}}^{(2)} = (1-p)^2 \mathcal{R}_{\text{GHZ}_N}^{(2)} - \max \mathcal{R}_{\rho_{k-\text{sep}}}^{(2)}$, where $\max \mathcal{R}_{\rho_{k-\text{sep}}}^{(2)}$ denotes the RHS of Eq. (30), such that the state $\rho_{\text{GHZ}}^{(N)}(p)$ just violates the respective k -separability bound. Now, it remains to determine the optimal total number of measurements $M_{\text{tot}}^{(\text{opt})}$ as demonstrated in Sec. B.2. The results of this calculation are presented in Fig. 4 of the main text for the detection of different degrees of multiparticle entanglement, i.e., violation of k -separability, and the discrimination of W -class entanglement, according to criterion (20), for different values of the noise parameter p and the number of qubits N .

Lastly, we give the precise measurement numbers required for the entanglement depth detection discussed in the last section of the maintext. There we considered GHZ states of $N = 11$ and $N = 20$ qubits, with fidelities taken according to recent experiments reported in Ref. [32]. The number of required measurements, in order to prove with a confidence of 90% that a GHZ state of $N = 11$ qubits and fidelity $F = 0.76$ has an entanglement depth of 5 or 7, is:

$$M_{\text{tot}}^{(\text{opt})} = (M \times K)^{(\text{opt})} = 3685 \times 125 \approx 4.60625 \times 10^5, \quad (67)$$

$$M_{\text{tot}}^{(\text{opt})} = (M \times K)^{(\text{opt})} = 571082 \times 105 \approx 5.996361 \times 10^7, \quad (68)$$

respectively. Furthermore, to prove entanglement depth 4 or 5, respectively, of a GHZ state of $N = 20$ qubits and fidelity $F = 0.44$ one requires

$$M_{\text{tot}}^{(\text{opt})} = (M \times K)^{(\text{opt})} = 11062 \times 4875 \approx 5.392725 \times 10^7, \quad (69)$$

$$M_{\text{tot}}^{(\text{opt})} = (M \times K)^{(\text{opt})} = 18752 \times 4420 \approx 8.288384 \times 10^7. \quad (70)$$

As explained previously the above numbers are based on the analytically determined optimal ratio between M and K for the respective type of entanglement under consideration.

We note that in Ref. [32] the number of performed measurements used to estimate the lower bounds on the fidelity is given by $(2N + 2) \times 16384$. While the latter numbers are only one to two orders of magnitude smaller than those reported in Eq. (67)-(70), the corresponding experimental procedure, based on a quantum sensing circuit, is considerably more involved. Furthermore, our method requires stabilization of the experiment only for the time of performing K measurements of a single randomly chosen measurement setting which might be of a general advantage in experiments based on Rydberg atom arrays or superconducting qubits. Lastly, we emphasize that our methods reveal informations about the entanglement structure of the states also in regimes of low fidelities where fidelity-based witnesses cannot give any insight. This is due to the fact that fidelity values of $F \leq 1/2$ can always be reproduced by fully separable states.

[1] C. D. Bruzewicz, J. Chiaverini, R. McConnell, and J. M. Sage, *Applied Physics Reviews* **6**, 021314 (2019).
[2] F. Arute, et al., *Nature* **574**, 505 (2019).
[3] M. Kjaergaard, M. E. Schwartz, J. Braumüller, P. Krantz, Philip and J. I. -J. Wang, S. Gustavsson, and W. D. Oliver, *Annu. Rev. Condens. Matter Phys.* **11**, 369 (2020).
[4] D. Gottesman, *Phys. Rev. A* **57**, 127 (1998).
[5] J. Preskill, *Introduction to Quantum Computation* (World Scientific, Singapore, 1998), pp. 213–269.
[6] J. Eisert, D. Hangleiter, N. Walk, I. Roth, D. Markham, R. Parekh, U. Chabaud, and E. Kashefi, *Nat. Rev. Phys.* **2**, 382 (2020).
[7] O. Gühne, and G. Tóth, *Phys. Rep.* **474**, 1 (2009).
[8] I. Šupić and J. Bowles, *Quantum* **4**, 337 (2020).
[9] R. D. Somma, J. Chiaverini, and D. J. Berkeland, *Phys. Rev. A* **74**, 052302 (2006).
[10] O. Gühne, C.-Y. Lu, W.-B. Gao, and J.-W. Pan, *Phys. Rev. A* **76**, 030305 (2007).
[11] R. Blume-Kohout, *New J. Phys.* **12**, 043034 (2010).
[12] D. Gross, Y.-K. Liu, S. T. Flammia, S. Becker, and J. Eisert, *Phys. Rev. Lett.* **105**, 150401 (2010).
[13] S. T. Flammia and Y.-K. Liu, *Phys. Rev. Lett.* **106**, 230501 (2011).

- [14] S. Aaronson, in Proceedings of the 50th Annual ACM SIGACT Symposium on Theory of Computing, (ACM, New York, 2018).
- [15] H.-Y. Huang, R. Kueng, and J. Preskill, *Nature Physics* **16**, 1050 (2020).
- [16] S. J. van Enk and C. W. J. Beenakker, *Phys. Rev. Lett.* **108**, 110503 (2012).
- [17] M. C. Tran, B. Dakić, F. Arnault, W. Laskowski, and T. Paterek, *Phys. Rev. A* **92**, 050301(R) (2015).
- [18] M. C. Tran, B. Dakić, W. Laskowski, and T. Paterek, *Phys. Rev. A* **94**, 042302 (2016).
- [19] A. Ketterer, N. Wyderka, and O. Gühne, *Phys. Rev. Lett.* **122**, 120505 (2019).
- [20] A. Ketterer, N. Wyderka, and O. Gühne, *Quantum* **4**, 325 (2020).
- [21] M. Krebsbach, Bachelor thesis, Albert-Ludwigs-Universität Freiburg (2019); <https://freidok.uni-freiburg.de/data/150706>.
- [22] A. Elben, B. Vermersch, M. Dalmonte, J. I. Cirac, and P. Zoller, *Phys. Rev. Lett.* **120**, 050406 (2018).
- [23] B. Vermersch, A. Elben, M. Dalmonte, J. I. Cirac, and P. Zoller, *Phys. Rev. A* **97**, 023604 (2018).
- [24] T. Brydges, A. Elben, P. Jurcevic, B. Vermersch, C. Maier, B. P. Lanyon, P. Zoller, R. Blatt, C. F. Roos, *Science* **364**, 260 (2019).
- [25] A. Elben, B. Vermersch, C. F. Roos, P. Zoller, *Phys. Rev. A* **99**, 052323 (2019).
- [26] V. Saggio, A. Dimić, C. Greganti, L. A. Rozema, P. Walther, B. Dakić, *Nat. Phys.* **15**, 935 (2019).
- [27] L. Knips, J. Dziewior, W. Kłobus, W. Laskowski, T. Paterek, P. J. Shadbolt, H. Weinfurter, and J. D. A. Meinecke, *npj Quantum Information* **6**, 51 (2020).
- [28] A. Elben, B. Vermersch, R. van Bijnen, C. Kokail, T. Brydges, C. Maier, M. K. Joshi, R. Blatt, C. F. Roos, and P. Zoller, *Phys. Rev. Lett.* **124**, 010504 (2020).
- [29] A. Elben, R. Kueng, H.-Y. Huang, R. van Bijnen, C. Kokail, M. Dalmonte, P. Calabrese, B. Kraus, J. Preskill, P. Zoller, B. Vermersch, *Phys. Rev. Lett.* **125**, 200501 (2020).
- [30] S. Imai, N. Wyderka, A. Ketterer, and O. Gühne, arXiv:2010.08372.
- [31] L. Knips, *Quantum Views* **4**, 47 (2020).
- [32] K. X. Wei *et al.*, *Phys. Rev. A* **101**, 032343 (2020).
- [33] A. Omran *et al.*, *Science* **365**, 570 (2020).
- [34] C. Song *et al.*, *Science* **365**, 574 (2020).
- [35] H. Aschauer, J. Calsamiglia, M. Hein, and H. J. Briegel, *Quantum Inf. Comput.* **4**, 383 (2004).
- [36] J. I. de Vicente and M. Huber, *Phys. Rev. A* **84**, 062306 (2011).
- [37] P. Badziag, C. Brukner, W. Laskowski, T. Paterek, and M. Żukowski, *Phys. Rev. Lett.* **100**, 140403 (2008).
- [38] W. Laskowski, M. Markiewicz, T. Paterek, and M. Żukowski, *Phys. Rev. A* **84**, 062305 (2011).
- [39] F. Mintert, M. Kus, and A. Buchleitner, *Phys. Rev. Lett.* **95**, 260502 (2005).
- [40] A. S. Sørensen and K. Mølmer, *Phys. Rev. Lett.* **86**, 4431 (2001).
- [41] O. Gühne, G. Tóth, and H.J. Briegel, *New J. Phys.* **7**, 229 (2005).
- [42] N. Wyderka and O. Gühne, *J. Phys. A: Math. Theor.* **53**, 345302 (2020).
- [43] C. Eltschka and J. Siewert, *Quantum* **4**, 229 (2020).
- [44] K. D. Schmidt, *Maß und Wahrscheinlichkeit*, (Springer-Verlag, Heidelberg, 2011).
- [45] C. Song *et al.*, *Phys. Rev. Lett.* **119**, 180511 (2017).
- [46] R. H. Hardin, N. J. A. Sloane, *Discrete & Computational Geometry* **15**, 429 (1996).
- [47] A. Ketterer and O. Gühne, *Phys. Rev. Research* **2**, 023130 (2020).
- [48] R. Potts, *Aust. J. Phys.* **6**, 498 (1953).